Biodegradation (2007) 18:675–692
DOI 10.1007/s10532-007-9101-2

ORIGINAL PAPER

A biogeochemical framework for metal detoxification in sulfidic systems

Alex O. Schwarz · Bruce E. Rittmann

Received: 23 August 2006 / Accepted: 1 January 2007 / Published online: 3 February 2007

Abstract We develop a comprehensive biogeochemical framework for understanding and quantitatively evaluating metals bio-protection in sulfidic microbial systems. We implement the biogeochemical framework in CCBATCH by expanding its chemical equilibrium and biological sub-models for surface complexation and the formation of soluble and solid products, respectively. We apply the expanded CCBATCH to understand the relative importance of the various key ligands of sulfidic systems in Zn detoxification. Our biogeochemical analysis emphasizes the relative importance of sulfide over other microbial products in Zn detoxification, because the sulfide yield is an order of magnitude higher than that of other microbial products, while its reactivity toward metals also is highest. In particular, metal-titration simulations using the expanded CCBATCH in a batch mode illustrate how sulfide detoxifies Zn, controlling its speciation as long as total sulfide is greater than added Zn. Only in the absence of sulfide does complexation of Zn to biogenic organic ligands play a role in detoxification. Our biogeochemical analysis conveys fundamental insight on the potential of the key ligands of sulfidic systems to effect Zn detoxification. Sulfide stands out for its reactivity and prevalence in sulfidic systems.

Keywords Biogeochemical model · Bio-protection · Metal speciation · Metal detoxification · Sulfidic systems · Toxic metals

A. O. Schwarz (✉)
Department of Civil Engineering, University of Concepción, Casilla 160-C, Correo 3, Ciudad Universitaria, Concepción, Chile
e-mail: alexschwarz@udec.cl

B. E. Rittmann
Center for Environmental Biotechnology, Biodesign Institute at Arizona State University, 1001 South McAllister Ave., Tempe, AZ 85287-5701, USA
e-mail: Rittmann@asu.edu

A. O. Schwarz · B. E. Rittmann
Department of Civil and Environmental Engineering, Northwestern University, 2145 Sheridan Road, Evanston, IL 60208-3109, USA

Introduction

We report on the development of a computational tool to represent complex biogeochemical systems and its application to bacterial communities involving sulfate-reducing bacteria (SRB). Our main goal is to understand quantitatively the role SRB play in metal-contaminated sites, because SRB can affect the chemical state of metals in ways that decrease or increase the availability of metals to living systems. Decreasing availability is especially important, because

this capacity can be harnessed to detoxify the contaminated water, the goal in bioremediation applications.

Bacterial communities involving SRB have great potential to detoxify metals naturally. Sulfide, the end product of sulfate reduction, forms sparingly soluble complexes with many toxic metals. Additionally, SRB can effect the direct and indirect reductive precipitation of metals. In direct reductive precipitation, SRB reduce metals enzymatically, leading to their precipitation as oxides, phosphates, or carbonates. For example, *Desulfovibrio desulfuricans* can couple the oxidation of hydrogen or simple organic acids to reduction of Fe(III), U(VI), Cr(VI), Tc(VII), Mo(VI), and Pd(II) (Lloyd et al. 2001), and *Desulfotomaculum reducens* can even grow with Cr(VI), Mn(IV), Fe(III), and U(VI) as electron acceptors (Tebo et al. 1998). In indirect reductive precipitation, a metabolite (i.e., sulfide) and not enzymes, acts as metal reductant (De Filippi 2000; Kim et al. 2001). Furthermore, sulfate reduction generates alkalinity, resulting in the further precipitation of metals as hydroxides (White and Gadd 1998). Not surprisingly then, several SRB-based technologies for metal bioremediation have been proposed and even implemented at full scale (Barnes et al. 1991; Benner et al. 1999; Webb et al. 1998; White et al. 1998; Rittmann et al. 2002a; Songkasiri et al. 2002, 2004).

Bacterial communities have the potential to act collectively to detoxify a metal. One such collective action is what we term *bio-protection*, in which one community member protects the entire community from metal toxicity by reducing toxic-metal bioavailability (Schwarz and Rittmann 2006). SRB are great candidates to provide anaerobic communities the necessary bio-protection from metals.

In order to understand how metal bioremediation, detoxification, and bio-protection ought to work in sulfidic systems, it is necessary to describe explicitly the interactions among bacterial populations, their metabolism, the speciation of the toxic metals, and the speciation of the complexing ligands; in other words, it is necessary to comprehensively describe the biogeochemistry of the system. We list next and illustrate in Fig. 1 the key biogenic components of our model sulfidic system and provide short explanations for why they need to be included and, in some cases, are very novel contributions:

- The active biomass has three distinct types: fermentative bacteria, H_2-utilizing SRB (H_2-SRB), and acetate-utilizing SRB (acetate-SRB). All three types are essential for full mineralization of a complex organic like glucose or lactate in an anaerobic setting. Only two of the three reduce sulfate, but the fermenting bacteria provide the substrate to drive sulfate reduction. The active biomass also has surface functional groups that can complex with metals.
- All types of active biomass generate inert biomass and extracellular polymeric substances (EPS). While not metabolically active, they contain complexing ligands that are part of the solid (non-mobile) phase. Adding these solid-phase ligands is novel for biogeochemical modeling.
- The active biomass also generates soluble microbial products (SMP) made up of utilization-associated products (UAP) and biomass-associated products (BAP). These are mobile complexing ligands produced by the bacteria. Having mobile, biogenic ligands is also novel for biogeochemical modeling.
- Sulfide is the reduced product from the two sulfate reducers (denoted L in Fig. 1). Sulfide

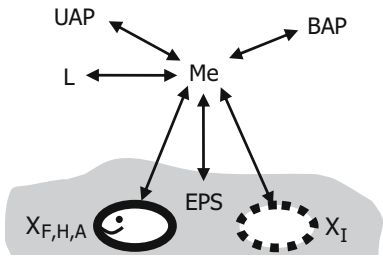

Fig. 1 Schematic of metal reactivity with biological components. The metal (Me) can be associated with solids (active cells of fermenting bacteria (X_F), H_2–SRB (X_H), and acetate-SRB (X_A), inert biomass (X_I) and extracellular polymeric substances (EPS)) through surface-complexation or precipitation reactions; and with soluble ligands (utilization-associated products (UAP), biomass-associated products (BAP), and other soluble biogenic ligands (L) such as sulfide)

forms well-known and strong complexes with metals.

In summary, we include the more-or-less ''usual'' ligands—sulfide and active biomass—but we add in new features of non-active biomass ligands, mobile biogenic ligands, and sub-division of the active bacteria into those that do or do not reduce sulfate to sulfide.

To describe all the interactions, we utilize the comprehensive biogeochemical portrayal possible in the numerical model CCBATCH (Rittmann and Van Briesen 1996; Banaszak et al. 1998; Van Briesen and Rittmann 1999, 2000; Van Briesen et al. 2000; Willett and Rittmann 2003). In brief, we insert the stoichiometry and kinetics of relevant reactions into the mass balance equations that CCBATCH uses to update the concentrations of chemical species. Because CCBATCH tracks the concentrations of all species, we can distinguish among the different metal-detoxification mechanisms, including bioprecipitation and complexation by the various ligands of biotic origin. Using CCBATCH with this full description, however, required that we add to CCBATCH the following major new features:

- An expanded chemical equilibrium sub-model that allows CCBATCH to represent adsorption reactions using surface-complexation theory and takes into account surface-charge effects using double-layer theory.
- An expanded biological sub-model that allows CCBATCH to represent a microbial community made of two or more microbial species and that includes the production and consumption of EPS, UAP, and BAP.

Using the expanded CCBATCH, we provide a comprehensive biogeochemical description for a sulfidogenic system having zinc as the toxic metal. Our key assumptions are:

- Bacterial sulfate reduction is the only sulfide source.
- The sulfate-reducing consortium comprises the 3 bacterial populations: fermentative bacteria, H_2-SRB, and acetate-SRB.
- The unified theory for microbial products (Laspidou and Rittmann 2002a, b) is used to quantify the relationships among the soluble (i.e., UAP, BAP) and solid (i.e., active cells, EPS, inert biomass) reactive ligand sources other than sulfide.
- Sulfide is the only reactive S species toward Zn, and it forms Zn–S complexes.
- An electrostatic surface-complexation model (Yee and Fein 2001) is used to describe metal complexation by active cells and inert biomass, which are solids.
- A non-electrostatic surface-complexation model (Liu and Fang 2002) is used to describe metal complexation by EPS. We assume that EPS and BAP exhibit similar binding characteristics.
- Malonate is used as a surrogate to describe the complexation behavior of UAP (Kuo and Parkin 1996).

The biogeochemical description follows a logical sequence. First, we explain the stoichiometry and kinetics of production of reactive ligands by the microbial species. Second, we define the reactivity of these ligands toward Zn, which sets the stage for determining the distribution or speciation of Zn among pools of different reactivity and elucidating how the Zn pools elicit a toxic response from the microorganisms. Third, we use our biogeochemical model to carry out titration-experiment simulations to understand the relative importance of the various key ligands of sulfidic systems in Zn detoxification.

We detail the transport processes involved in the movement of metals in aqueous systems in a companion paper (Schwarz and Rittmann 2007); transport resistance is responsible for the formation of chemical gradients, a hypothesized bio-protection mechanism (Schwarz and Rittmann 2006).

Stoichiometry and kinetics of reactive-ligand generation in sulfidic systems

Sulfate-reducing bacteria use low-molecular-weight compounds as electron donors and, therefore, depend on fermentative bacteria that degrade the original, more complex forms from

dissolved or particulate organic matter. Hydrogen and acetate are the key fermentation products through which reducing equivalents of organic matter are channeled into methanogenesis and sulfate reduction (Madigan et al. 2000). SRB traditionally are divided in two broad physiological groups according to their ability to completely oxidize organic substrates. Incomplete oxidizers are distinguished by incomplete oxidation of their energy source to the level of acetate and by their ability to oxidize hydrogen. Complete oxidizers specialize in the oxidation of fatty acids, particularly acetate, all the way to carbon dioxide (Widdel 1988). Consequently, the mathematical representation of a sulfidic system requires, at a minimum, fermentative bacteria, SRB-complete oxidizers (acetate-SRB), and SRB-incomplete oxidizers (H_2-SRB).

We apply the unified modeling approach developed by Laspidou and Rittmann (2002a, b)—the unified theory for EPS, SMP, and active and inert biomass—to quantify the relationships among solid and soluble reactive-ligand sources in sulfidic systems. Fig. 2 illustrates the components and their relationships in the unified model. In the next section on speciation, we describe the reactivity of these ligand sources and sulfide toward Zn.

Table 1, which results from applying the unified theory of microbial products to each individual microbial population, indicates through stoichiometric expressions how the key bacteria-mediated processes affect the concentrations of solid and soluble products. Table 1 also lists kinetic expressions for these processes. Fermentative bacteria couple glucose utilization to production of active biomass X_F, EPS and UAP. The true-yield coefficient (Y_F) accounts for all organic products coming from substrate utilization, and the coefficients α_{Fi} indicate how the substrate electrons are diverted toward active biomass, formation of UAP, and formation of EPS. Additionally, the coefficient β expresses the fraction of substrate electrons that go to fermentation products that end up in acetate; the difference (1-β) ends up in hydrogen. Similarly, H_2-SRB and acetate-SRB couple, respectively, hydrogen oxidation and acetate oxidation with sulfate reduction to grow new biomass (X_H, X_A), and produce EPS and UAP.

The unified theory of bacterial products also assumes that, for each bacterial population, residual inert biomass X_I is produced from the decay of active biomass and that BAP are produced from the hydrolysis of EPS. We further assume that fermentative bacteria are able to grow with the soluble products UAP and BAP as electron donors, and that SRB, due to their more restricted substrate range, are not capable of UAP and BAP utilization. However, SRB do participate in the metabolism of UAP and BAP by utilizing the low-molecular-weight intermediates released from their fermentation.

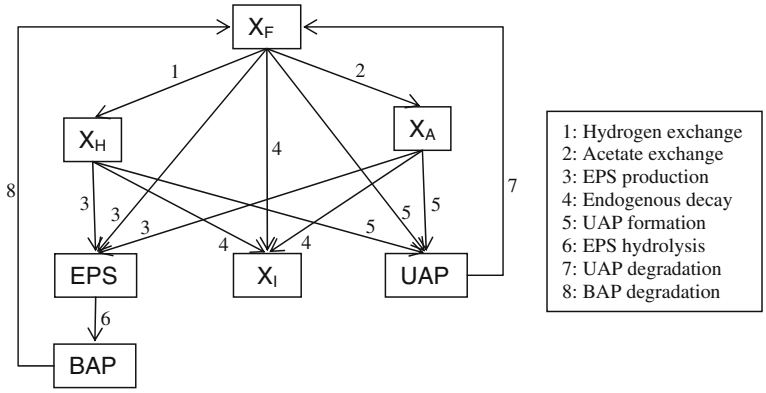

Fig. 2 Relationships among the soluble (i.e., UAP, BAP) and solid (i.e., active cells, EPS, inert biomass) microbial products. X_F is fermentative active biomass, X_H is H_2-SRB active biomass, X_A is acetate-SRB active biomass, EPS is extracellular polymeric substances, X_I is inert biomass, UAP is utilization-associated products, and BAP is biomass-associated products

Table 1 Matrix of stoichiometry and kinetic expressions used for the representation of a sulfidic system

Process name	Biomass types					SMP		Substrates				Sulfide	Kinetic expressions
	X_F	X_H	X_A	X_I	EPS	UAP	BAP	Gluc.	H_2	Acetate	Sulfate		
Fermenter metabolism	$\alpha_{F1}Y_F$				$\alpha_{F2}Y_F$	$\alpha_{F3}Y_F$		–1	$10(1-\beta)$ $(1.2-Y_F)$	2.5β $(1.2-Y_F)$			$\hat{q}_g \frac{C_g}{K_g + C_g} X_F$
Fermenter inactivation	–1			1									$(1-f_d)b_F X_F$
Fermenter respiration	–1								$10(1-\beta)$	2.5β			$f_d b_F X_F$
H_2-SRB metabolism		$\alpha_{H1}Y_H$			$\alpha_{H2}Y_H$	$\alpha_{H3}Y_H$			–1		–2.5 $(0.1-Y_H)$	2.5 $(0.1-Y_H)$	$\hat{q}_h \frac{C_h}{K_h + C_h} \frac{C_s}{K_{s,H} + C_s} X_H$
H_2-SRB inactivation		–1		1									$(1-f_d)b_H X_H$
H_2-SRB respiration		–1									–2.5	2.5	$f_d b_H \frac{C_s}{K_{s,H} + C_s} X_H$
Acetate-SRB metabolism			$\alpha_{A1}Y_A$		$\alpha_{A2}Y_A$	$\alpha_{A3}Y_A$				–1	–2.5 $(0.4-Y_A)$	2.5 $(0.4-Y_A)$	$\hat{q}_a \frac{C_a}{K_a + C_a} \frac{C_s}{K_{s,A} + C_s} X_A$
Acetate-SRB inactivation			–1	1									$(1-f_d)b_A X_A$
Acetate-SRB respiration			–1								–2.5	2.5	$f_d b_A \frac{C_s}{K_{s,A} + C_s} X_A$
BAP formation					–1		1						k_{hyd} EPS
Fermenter UAP degradation	Y_{PF}					–1			$10(1-\beta)(1-Y_{PF})$	$2.5\beta(1-Y_{PF})$			$\hat{q}_{UAP} \frac{UAP}{K_{UAP} + UAP} X_F$
Fermenter BAP degradation	Y_{PF}						–1		$10(1-\beta)(1-Y_{PF})$	$2.5\beta(1-Y_{PF})$			$\hat{q}_{BAP} \frac{BAP}{K_{BAP} + BAP} X_F$

Table 2 Parameter definitions and units for the matrix of stoichiometry and kinetic expressions

Parameter	Definition	Units[a]
α_{F1}, α_{F2}, α_{F3}	Fermenting bacteria yield coefficient for cells, EPS and UAP respectively	–
α_{A1}, α_{A2}, α_{A3}	Acetate-SRB yield coefficient for cells, EPS and UAP respectively	–
α_{H1}, α_{H2}, α_{H3}	H_2-SRB yield coefficient for cells, EPS and UAP respectively	–
β	Fraction of electrons going to fermentation products than end up in acetate	–
b_F, b_A, b_H	First-order endogenous decay rate coefficient of fermenting bacteria, acetate-SRB, and H_2-SRB respectively	T^{-1}
BAP	Concentration of BAP	M_pL^{-3}
C_a	Concentration of acetate	M_aL^{-3}
C_g	Concentration of glucose	M_gL^{-3}
C_h	Concentration of hydrogen	M_hL^{-3}
C_s	Concentration of sulfate	M_sL^{-3}
EPS	Concentration of EPS	M_xL^{-3}
f_d	Biodegradable fraction of active biomass	–
k_{hyd}	First-order hydrolysis rate coefficient	T^{-1}
K_{BAP}	Half-maximum-rate concentration for BAP utilization	M_pL^{-3}
K_{UAP}	Half-maximum-rate concentration for UAP utilization	M_pL^{-3}
K_a	Half-maximum-rate concentration for utilization of acetate	M_aL^{-3}
K_g	Half-maximum-rate concentration for utilization of glucose	M_gL^{-3}
K_h	Half-maximum-rate concentration for utilization of hydrogen	M_hL^{-3}
$K_{s,\ A}$	Half-maximum-rate concentration for utilization of sulfate of acetate-SRB	M_sL^{-3}
$K_{s,\ H}$	Half-maximum-rate concentration for utilization of sulfate of H_2-SRB	M_sL^{-3}
$\hat{q}_g$	Maximum specific glucose utilization rate	$M_gM_x^{-1}T^{-1}$
$\hat{q}_a$	Maximum specific acetate utilization rate	$M_aM_x^{-1}T^{-1}$
$\hat{q}_h$	Maximum specific hydrogen utilization rate	$M_hM_x^{-1}T^{-1}$
$\hat{q}_{BAP}$	Maximum specific BAP utilization rate	$M_pM_x^{-1}T^{-1}$
$\hat{q}_{UAP}$	Maximum specific UAP utilization rate	$M_pM_x^{-1}T^{-1}$
UAP	Concentration of UAP	M_pL^{-3}
X_A	Concentration of active biomass of acetate-SRB	M_xL^{-3}
X_F	Concentration of active biomass of fermenting bacteria	M_xL^{-3}
X_H	Concentration of active biomass of H_2-SRB	M_xL^{-3}
X_I	Concentration of true residual inert biomass	M_xL^{-3}
Y_F	True yield for glucose utilization	$M_xM_g^{-1}$
Y_H	True yield for hydrogen utilization	$M_xM_h^{-1}$
Y_A	True yield for acetate utilization	$M_xM_a^{-1}$
Y_{PF}	True yield for SMP utilization	$M_xM_p^{-1}$

[a] For implementation in CCBATCH, all mass (M) is in moles, volume (L^3) is liters, and time (T) is days. Subscripts are a for acetate, g for glucose, h for hydrogen, s for sulfate, p for UAP and BAP, and x for active biomass, residual inert biomass and EPS

Additionally, substrate-utilization rates according to the unified theory are based on Monod (or multiplicative-Monod) kinetics; rates of inactivation or formation of inert biomass are proportional to the endogenous decay rate (e.g., $b_H X_H$ for fermentative bacteria) multiplied by the non-biodegradable fraction of the active biomass ($1 - f_d$); rates of endogenous respiration of biomass are proportional to the endogenous decay rate multiplied by the biodegradable fraction of the active biomass f_d and a Monod-term denoting electron acceptor limitation, if warranted; and, the rate of BAP formation is proportional to EPS concentration. Table 2 defines parameters used in the model formulation, as well as their units.

We use the fermentative bacteria as an example to explain how electron mass balances are used to determine the stoichiometric coefficients in Table 1. The first step is to determine the electron equivalents associated with the oxidation or reduction of the key chemical species (i.e., biomass types, SMP, and substrates) from reduction half-reactions that are in the format listed in Rittmann and McCarty (2001). Thus, fermentative bacteria utilize electrons

from glucose (24 e^- eq/mol) for synthesis of new biomass ($C_5H_7O_2N$, having 20 e^- eq/mol with ammonium as nitrogen source) and for energy production (the fermentation products hydrogen and acetate accept 2 e^- eq/mol and 8 e^- eq/mol respectively).

The cell synthesis half-reaction uses the empirical formula $C_5H_7O_2N$ to represent the composition of new microbial cells. In the model, we use the same empirical formula for SMP, inerts, and EPS, since they come from active biomass. The key intermediates of anaerobic food webs are acetate and hydrogen, and the relative proportion of these reduced fermentation products is determined in the model using the parameter β. Glucose fermentation with a relative product proportion of 2 mol of hydrogen per mole of acetate yields the greatest amount of energy with 4 ATP/hexose (Fenchel and Finlay 1995). This fermentation is carried out by *Clostridium pasteurianum* if the hydrogen pressure is kept below 10^{-4}atm. In this case, 67% of the electrons shuttled to products end up in acetate ($\beta = 0.67$), with the other 33% in H_2. Written in terms of the true yield, the fraction of electrons used for energy generation is

$$1 - \frac{20}{24}\frac{\frac{e^-eq}{mol-cells}}{\frac{e^-eq}{mol-glucose}} Y_F \frac{mol-cells}{mol-glucose} \quad (1)$$

Hence, the stoichiometric factor for acetate production is

$$\left(1 - \frac{20}{24}\frac{\frac{e^-eq}{mol-cells}}{\frac{e^-eq}{mol-glucose}} Y_F \frac{mol-cells}{mol-glucose}\right) \times \beta \frac{24}{8}\frac{\frac{e^-eq}{mol-glucose}}{\frac{e^-eq}{mol-acetate}} = 2.5\beta(1.2 - Y_F)\frac{mol-acetate}{mol-glucose} \quad (2)$$

And, the stoichiometric factor for hydrogen production is

Table 3 Parameter values for the matrix of stoichiometry and kinetic expressions for a sulfidigenic system

Parameter	Values in mol units	Source
α_{F1}, α_{F2}, α_{F3}	0.53, 0.37, 0.1, respectively	Laspidou and Rittmann 2002b
α_{A1}, α_{A2}, α_{A3}	0.53, 0.37, 0.1, respectively	Laspidou and Rittmann 2002b
α_{H1}, α_{H2}, α_{H3}	0.53, 0.37, 0.1, respectively	Laspidou and Rittmann 2002b
β	0.67	Fenchel and Finlay 1995
b_F, b_A, b_H	0.05 d^{-1}	Rittmann and McCarty 2001
f_d	0.8	Rittmann and McCarty 2001
k_{hyd}	0.17 d^{-1}	Laspidou and Rittmann 2002b
K_a	1.24×10^{-4} mol-acetate/l	Widdel 1988[a]
K_g	1.0×10^{-4} mol-glucose/l	Assumed
K_h	1.6×10^{-6} mol-hydrogen/l	Widdel 1988[b]
$K_{s,\ A}$	2.16×10^{-4} mol-sulfate/l	Widdel 1988[c]
$K_{s,\ H}$	1.86×10^{-5} mol-hydrogen/l	Widdel 1988[d]
$\hat{q}_g$	5.74 mol-glucose/(mol-cells d)	Rittmann and McCarty 2001[c]
$\hat{q}_a$	15.35 mol-acetate/(mol-cells d)	Rittmann and McCarty 2001[c]
$\hat{q}_h$	59.47 mol-hydrogen/(mol-cells d)	Rittmann and McCarty 2001[c]
$\hat{q}_{BAP}/K_{BAP}$	271.2 l/(mol-cells d)	Noguera et al. 1994[d]
$\hat{q}_{UAP}/K_{UAP}$	35.03 l/(mol-cells d)	Noguera et al. 1994[d]
Y_F	0.2108 mol-cells/mol-glucose	Table 6
Y_H	0.0299 mol-cells/mol-hydrogen	Table 6
Y_A	0.0327 mol-cells/mol-acetate	Table 6
Y_{PF}	0.2 mol-cells/mol-SMP	Assumed

[a] Average for *Desulfobacter postgatei*

[b] Average for *Desulfovibrio vulgaris*

[c] Assuming an electron flow to the energy reaction of 1 e^- eq/gVSS-d

[d] SMP degradation kinetics is described by first-order expressions for UAP and BAP

$$\left(1-\frac{20}{24}\frac{\frac{e^-eq}{mol-cells}}{\frac{e^-eq}{mol-glucose}}Y_F\frac{mol-cells}{mol-glucose}\right)\times(1-\beta)\frac{24}{2}\frac{\frac{e^-eq}{mol-glucose}}{\frac{e^-eq}{mol-hydrogen}}=10(1-\beta)(1.2-Y_F)\frac{mol-hydrogen}{mol-glucose} \quad (3)$$

Finally, Table 3 shows parameter values that we use with the matrix of stoichiometry and kinetic expressions in Table 1 for a sulfidogenic system. In addition to the notes at the bottom of Table 3, we make several critical assumptions that need further explanation. The yield coefficients determine how bacteria partition the flow of electrons coming from the substrate among several microbial products. This partitioning depends not only on the microbial species, but also on the physiological state of the microbes. The yield coefficients listed in Table 3 were determined by Laspidou and Rittmann (2002b), who successfully represented steady-state and batch growth of aerobic heterotrophs (Hsieh et al. 1994). Additionally, Laspidou and Rittmann (2002b) used a biomass yield of 0.45 mg_x/mg_p for aerobic utilization of SMP as an electron donor. Considering that typical yields of BOD utilization for aerobic heterotrophs are similar (0.42–0.49), using analogy, a value of Y_{PF} of 0.2 mg_x/mg_p, close to Y_F, appears reasonable for fermenting bacteria. Also, we assume a general half-maximum-rate concentration value for utilization of glucose of 1.0×10^{-4} mol glucose/l.

Zn speciation

It is firmly established that metal bioavailability and toxicity depend directly on the chemical forms in which the metals are present in solution (i.e., the metal's chemical speciation) (Allen and Hansen 1996; Gambrell 1994). For example, the availability and toxicity of many trace metals to planktonic microorganisms are determined by their free-ion concentration, rather than their total concentration; thus, availability and toxicity are often decreased by complexation (Morel and Hering 1993). Conceptual models including the Free Ion Activity Model (FIAM) (Campbell 1995; Morel and Hering 1993), the Biotic Ligand Model (BLM) (Campbell et al. 2002; Paquin et al. 2002), and the extended FIAM (Brown and Markich 2000) have been very successful predictors of metal bioavailability in a wide range of systems and conditions.

In sulfidic systems, hydrogen sulfide is often the dominant reactive sulfur species, and, therefore, for simplicity, our model includes Zn–H_2S complexes as the only Zn–S interactions. Additionally, we assume that the system is closed and has no gas phase. Table 4 shows the key coordination reactions for Zn^{2+} and H_2S, including acid–base, complex formation, and precipitation.

Precipitation and dissolution reactions are typically kinetically controlled, and the modeling of these reactions in microbial systems often is based on kinetic rate expressions that include the intrinsic kinetics for reaction or mass-transport control, the difference from thermodynamic equilibrium, and the aqueous concentration of the rate limiting metal or ligand (Rittmann et al. 2002b); however, precipitation of sulfide solids is extremely fast (Rickard 1995), such that the equilibrium approach could be valid. We use the equilibrium approach here.

Table 1 introduced microbial products, namely active biomass, inert biomass, EPS and SMP, and the microbially catalyzed reactions that result in their production and consumption. These microbial products have affinity toward metals due to the presence of functional groups with O, N, and S atoms; hence, they may significantly affect metal speciation (Stone 1997). Therefore, in order to understand the reactivity and fate of metals in microbial systems, the reactions involving microbial products and metals need to be elucidated.

Table 4 Zn–H_2S coordination reactions and parameters

Acid–base reactions:	
$H_2S \leftrightarrow HS^- + H^+$	$pK_{a1} = 7.02$
$HS^- \leftrightarrow S^{2-} + H^+$	$pK_{a2} = 17.3$
Complexation reactions:	
$Zn^{2+} + 2H_2S \leftrightarrow 2H^+ + Zn(HS)_2^0$	$\log K_1 = -1.22$
$Zn^{2+} + 4H_2S \leftrightarrow 4H^+ + Zn(HS)_4^{2-}$	$\log K_2 = -13.44$
$Zn^{2+} + 2H_2S \leftrightarrow 3H^+ + ZnS(HS)^-$	$\log K_3 = -7.23$
$Zn^{2+} + 3H_2S \leftrightarrow 4H^+ + ZnS(HS)_2^{2-}$	$\log K_4 = -14.94$
Sphalerite dissolution/precipitation:	
$ZnS_{(s)} + 2H^+ \leftrightarrow Zn^{2+} + H_2S$	$\log K_{sp} = -4.43$

Sources: Daskalakis and Helz (1993) and NIST (1998)

Despite differences in bacterial-envelope structure, a wide range of bacterial species exhibit similar metal-adsorption behavior (Yee and Fein 2001). Hence, a generalized adsorption model, independent of the species involved, can be used to predict metal adsorption onto bacterial surfaces. In particular, we use the generalized model developed by Yee and Fein (2001), based on the average characteristics of 9 Gram-positive and Gram-negative bacterial strains, to describe the acid–base and metal binding behavior of active cells. With active cells we mean intact cells, their EPS excluded. Also, we assume that the generalized model, developed using non-metabolizing viable bacterial cells, is valid for metabolic active cells and inerts. We use the generalized model with inerts, considering that a significant fraction of the inert biomass is remnants of cell wall components. Consideration of the generalized model to account for metal-microbe interactions required our addition to CCBATCH of a surface complexation routine that handles electrostatic interactions.

According to the generalized model, the negative charge of bacterial cell walls results from deprotonation of carboxyl, phosphoryl, and hydroxyl functional groups (Yee and Fein 2001):

$$\equiv \mathrm{X}-\mathrm{COOH}^0 \leftrightarrow \equiv \mathrm{X}-\mathrm{COO}^- + \mathrm{H}^+ \quad (4)$$

$$\equiv \mathrm{X}-\mathrm{PO_4H}^0 \leftrightarrow \equiv \mathrm{X}-\mathrm{PO_4^-} + \mathrm{H}^+ \quad (5)$$

$$\equiv \mathrm{X}-\mathrm{OH}^0 \leftrightarrow \equiv \mathrm{X}-\mathrm{O}^- + \mathrm{H}^+ \quad (6)$$

where $\equiv$X represents the bacterial cell wall to which functional groups are attached. Songkasiri (2003) and Cox et al. (1999) concluded, based on the average pK_a around 10 for reaction 6, that the identity of the functional group for that reaction is mainly amino and not hydroxyl, giving

$$\equiv \mathrm{X}-\mathrm{NH_3^+} \leftrightarrow \equiv \mathrm{X}-\mathrm{NH_2} + \mathrm{H}^+ \quad (7)$$

The pK_a ranges for hydroxyl and amino sites overlap and the high-pK_a site is probably a mixture of amino and hydroxyl sites. Furthermore, the exact identity of binding sites does not affect the validity or utility of the model; therefore, we continue to use hydroxyl sites as surrogates for both hydroxyl and amino sites.

The stability constants for the deprotonation reactions are, respectively,

$$K_1^{\mathrm{app}} = \frac{[\equiv \mathrm{X}-\mathrm{COO}^-]\{\mathrm{H}^+\}}{[\equiv \mathrm{X}-\mathrm{COOH}^0]} \quad (8)$$

$$K_2^{\mathrm{app}} = \frac{[\equiv \mathrm{X}-\mathrm{PO_4^-}]\{\mathrm{H}^+\}}{[\equiv \mathrm{X}-\mathrm{PO_4H}^0]} \quad (9)$$

$$K_3^{\mathrm{app}} = \frac{[\equiv \mathrm{X}-\mathrm{O}^-]\{\mathrm{H}^+\}}{[\equiv \mathrm{X}-\mathrm{OH}]} \quad (10)$$

where [ ] denotes the concentration of a surface species in moles per liter of solution, and { } denotes the activity of an aqueous species. The activity coefficients for protonated and deprotonated surface species are assumed to be equal (Dzombak and Morel 1990).

The interactions between zinc and the deprotonated surface sites are described by the stability reactions

$$\equiv \mathrm{X}-\mathrm{COO}^- + \mathrm{Zn}^{2+} \leftrightarrow \equiv \mathrm{X}-\mathrm{COOZn}^+ \quad (11)$$

$$\equiv \mathrm{X}-\mathrm{PO_4^-} + \mathrm{Zn}^{2+} \leftrightarrow \equiv \mathrm{X}-\mathrm{PO_4Zn}^+ \quad (12)$$

$$\equiv \mathrm{X}-\mathrm{O}^- + \mathrm{Zn}^{2+} \leftrightarrow \equiv \mathrm{X}-\mathrm{OZn}^+ \quad (13)$$

The stability constants for each reaction are

$$K_4^{\mathrm{app}} = \frac{[\equiv \mathrm{X}-\mathrm{COO}^-]\{\mathrm{Zn}^{2+}\}}{[\equiv \mathrm{X}-\mathrm{COOZn}^+]} \quad (14)$$

$$K_5^{\mathrm{app}} = \frac{[\equiv \mathrm{X}-\mathrm{PO_4^-}]\{\mathrm{Zn}^{2+}\}}{[\equiv \mathrm{X}-\mathrm{PO_4Zn}^+]} \quad (15)$$

$$K_6^{\mathrm{app}} = \frac{[\equiv \mathrm{X}-\mathrm{O}^-]\{\mathrm{Zn}^{2+}\}}{[\equiv \mathrm{X}-\mathrm{OZn}^+]} \quad (16)$$

Due to deprotonation of surface functional groups, bacterial cell walls acquire a negative charge, creating an electric field in its immediate vicinity. The interactions between the electric field and the adsorbing protons and metals can be quantified by correcting the equilibrium constants referenced to zero surface charge K^{int} using the following relationship

$$K_i^{app} = K_i^{int} e^{(-\Delta z F \Psi / RT)} \quad i = 1 \cdots 6 \tag{17}$$

where K_i^{int} and K_i^{app} are the intrinsic and apparent equilibrium constants, respectively, for the *i*th surface complexation reaction, F is the Faraday constant (9.649×10^4 coulombs mol^{-1}), Ψ the surface potential (volts), Δz the change in charge of the surface species for the reaction, R the gas constant (8.314 J mol^{-1} °K^{-1}), and T the absolute temperature (°K). In order to compute the surface potential Ψ, the generalized model defines the surface charge-potential relationship with the constant-capacitance (CC) model

$$\sigma = C\Psi \tag{18}$$

where σ is the surface charge (coulombs m^{-2}), and C the capacitance of the bacterial surface (farads m^{-2}).

Table 5 summarizes the reactions and parameters for zinc adsorption onto bacteria surfaces. Table 5 also shows the reactions describing the binding behavior of EPS and SMP. The majority of studies conducted to date demonstrate that EPS exhibit affinity for metals. However, the type of quantitative information needed by chemical equilibrium models, such as binding strengths and binding site densities, are generally not determined in these studies. As a first approximation, we assume that EPS and BAP exhibit similar binding characteristics, because EPS hydrolysis generates the high-MW BAP, according to the unified model of microbial products (Laspidou and Rittmann 2002a, b). EPS and BAP metal complexation is non-electrostatic, and we use the average pK_a values and site densities of EPS from a hydrogen-producing sludge and a sulfate-reducing biofilm (Liu and Fang 2002). Also, because no stability constants describing zinc binding to EPS or BAP are available in the literature, we use cell-wall affinities for zinc as surrogates.

UAP are small molecules derived from the original substrate and, therefore, exhibit distinctive metal binding properties. Our first approxi-

Table 5 Model reactions and parameters for zinc complexation by organic microbial products

Cell surface characteristics (Yee and Fein 2001):		
Density of ≡ X–COOH (carboxyl) sites on cell wall = 2×10^{-3} mol/g bacteria (dry wt)		
Density of ≡ X–PO_4H (phosphoryl) sites on cell wall = 0.8×10^{-3} mol/g bacteria (dry wt)		
Density of ≡ X–OH (hydroxyl) sites on cell wall = 1.7×10^{-3} mol/g bacteria (dry wt)		
Capacitance value = 8.0 F/m^2		
Surface complexation reactions:		
$\equiv X-COOH^0 \leftrightarrow \equiv X-COO^- + H^+$;	$\log K_1^{int} = -5.0$	(Yee and Fein 2001)
$\equiv X-PO_4H^0 \leftrightarrow \equiv X-PO_4^- + H^+$;	$\log K_2^{int} = -7.2$	(Yee and Fein 2001)
$\equiv X-OH^0 \leftrightarrow \equiv X-O^- + H^+$;	$\log K_3^{int} = -9.7$	(Yee and Fein 2001)
$\equiv X-COO^- + Zn^{2+} \leftrightarrow \equiv X-COOZn^+$;	$\log K_4^{int} = 3.4$	(Fein et al. 2001)
$\equiv X-PO_4^- + Zn^{2+} \leftrightarrow \equiv X-PO_4Zn^+$;	$\log K_5^{int} = 4.9$	(Fein et al. 2001)
EPS and BAP coordination sites characteristics (Liu and Fang 2002):		
Density of ≡ X–COOH (carboxyl) sites on EPS and BAP = 6.21×10^{-3} mol/g (dry wt)		
Density of ≡ X–PO_4H (phosphoryl) sites on EPS and BAP = 0.53×10^{-3} mol/g (dry wt)		
Density of ≡ X–OH(hydroxyl) sites on EPS and BAP = 6.93×10^{-3} mol/g (dry wt)		
Non-electrostatic model		
EPS and BAP complexation reactions:		
$\equiv X-COOH^0 \leftrightarrow \equiv X-COO^- + H^+$;	$\log K_1 = -4.89$	(Liu and Fang 2002)
$\equiv X-PO_4H^0 \leftrightarrow \equiv X-PO_4^- + H^+$;	$\log K_2 = -7.30$	(Liu and Fang 2002)
$\equiv X-OH^0 \leftrightarrow \equiv X-O^- + H^+$;	$\log K_3 = -10.56$	(Liu and Fang 2002)
$\equiv X-COO^- + Zn^{2+} \leftrightarrow \equiv X-COOZn^+$;	$\log K_4 = 3.4$	(Fein et al. 2001)
$\equiv X-PO_4^- + Zn^{2+} \leftrightarrow \equiv X-PO_4Zn^+$;	$\log K_5 = 4.9$	(Fein et al. 2001)
UAP coordination sites characteristics (Kuo and Parkin 1996):		
Density of COOH (carboxyl) sites on UAP = 2.49×10^{-3} mol/g (dry wt)		
UAP complexation reactions:		
$\equiv X-COOH^0 \leftrightarrow \equiv X-COO^- + H^+$;	$\log K_1 = -5.7$	(Stumm and Morgan 1996)
$\equiv X-COO^- + Zn^{2+} \leftrightarrow \equiv X-COOZn^+$;	$\log K_2 = 3.8$	(Stumm and Morgan 1996)

Sources: Yee and Fein 2001; Fein et al. 2001; Liu and Fang 2002; Kuo and Parkin 1996; and Stumm and Morgan 1996

mation is to use malonate as a surrogate for UAP metal complexation, with an average complexation capacity of 2.49 mmol/g UAP (dry wt) (Kuo and Parkin 1996).

Songkasiri et al. (2002) provide the first comprehensive bio-sorption study to simultaneously quantify sorption to EPS, cell walls, and whole cells. Their specific model system involved association between the actinide neptunium and the bacterium *Shewanella alga*. pK_a values for *S. alga* whole cells, purified cell walls, and EPS were generally similar and comparable to values listed in Table 5. On the other hand, the specific site concentrations of *S. alga* differ in significant ways. First, the total-cell-wall site density of *S. alga* was three times greater than the total site density for intact cells of the generalized model. This difference seems reasonable, considering that the cytoplasm of intact cells is generally not available for association with metals. The purified cell wall results suggest that the site densities of inerts might be significantly higher than the site densities of intact (active) cells, considering that all the dry mass of inerts is available for association with metals. Second, the EPS total-site density of *S. alga* is about one half the EPS total-site density determined by Liu and Fang (2002). The variability of EPS results probably is due to the variability in EPS composition. The polysaccharide content in EPS varies from 40% to 95%, while the protein content range is <1–60% (Flemming and Wingender 2001).

Although EPS and BAP might have similar binding behaviors, EPS is a solid and BAP is soluble; hence, they are treated as immobile (EPS) and mobile (BAP) by the model. Additionally, while UAP and BAP are soluble, they probably have different binding behaviors, because they originate from different processes and starting materials.

Biogeochemical analysis

The goal of the biogeochemical analysis of sulfidic systems presented here is to gain a fundamental understanding of the potential and relative importance of various ligands of biotic origin in metal detoxification. This analysis integrates the information on microbiology and speciation presented previously and takes advantages of the expanded sub-models in CCBATCH. We couple transport processes and biogeochemical reactivity in the companion paper (Schwarz and Rittmann 2007). Therefore, as part of this preliminary analysis, we answer the following question: *What is the relative importance of complexation by active cells, inerts, EPS, SMP, and sulfide, in metal detoxification?*

We write a balanced reaction for the anaerobic metabolism of 1 mol of glucose to gain insight into the reactant and product dynamics of microbial reactions in sulfidic systems. We take into account reaction energetics to determine the true yield coefficients Y_F, Y_H, and Y_A, which are key parameters of the matrix of stoichiometry listed in Table 1. The procedure of balancing microbial reactions is detailed in Rittmann and McCarty (2001) and is not repeated here. During metabolism, bacteria convert electrons originating from the electron donor into cells. This cell synthesis reaction demands energy, which bacteria generate in a second reaction by shunting the remaining electrons originating from the electron donor to an electron acceptor. The key to determining the true yield is then to partition the electron flow coming from the electron donor in order to balance energy needs for synthesis, and energy production. We performed yield calculations for the three microbial populations and used this information to create the microbial reactions presented in Table 6.

In terms of the bio-protection concept and the capacity of this microbial system to interact with metals, three aspects are critical. First, according to the sum-of-steps line, one mole of glucose results in ~0.36 mol of cells, which includes active cells, EPS, and UAP. Glucose, a non-reactive compound, is transformed into a series of microbial products with reactivity toward metals. Second, sulfidogenesis results in ~2.1 mol of hydrogen sulfide per mole of glucose consumed, and hydrogen sulfide possesses high reactivity toward toxic metals. Third, ~3.9 mol of alkalinity are generated per mole glucose consumed, and this affects the pH and, hence, metal speciation.

The stoichiometry of microbial-product generation can be used with the site-density information

Table 6 Stoichiometric coefficients for steps in the degradation of glucose in sulfidic systems[a]

Step	Glucose	H_2	Ac^-	SO_4^{2-}	H_2S	H^+	H_2O	H_2CO_3	NH_4^+	$C_5H_7O_2N$
Glucose to hydrogen and acetate	–1	3.2974	1.6487	0	0	1.8595	–2.6651	1.6487	–0.2108	0.2108
Hydrogen oxidation	0	–1	–0.0498	–0.2251	0.2251	–0.4701	1.0897	–0.0498	–0.0299	0.0299
Acetate mineralization	0	0	–1	–0.9183	0.9183	–2.8038	0.0981	1.8365	–0.0327	0.0327
Sum of steps	–1	0	0	–2.1055	2.1055	–3.8528	1.0737	4.2108	–0.3579	0.3579

[a] Assumptions: ammonium is the nitrogen source in all synthesis reactions; in glucose fermentation, $\beta = 0.67$; and, in hydrogen mineralization, 67% of the carbon for synthesis comes from acetate and 33% from H_2CO_3

to assess the relative importances of several ligand types in detoxification. Table 7 shows that 1 mol of glucose yields 2.28 mol of reactive ligands in a model sulfidogenic system, assuming that reactive sites on active cells, EPS and SMP include carboxyl and phosphoryl sites only. The sulfide yield is an order of magnitude higher than other yields, while the yields of EPS and active cells are similar.

We now compare the detoxification potential of the key ligands by simulating a metal titration using the comprehensive biogeochemical representation possible in the expanded CCBATCH. This is a comprehensive approach, because it takes into account reactive-ligand concentration, as well as reactivity. To simulate the metal titrations, we use CCBATCH in a non-kinetic batch mode, with input of equilibrium reactions only (i.e., acid–base, surface complexation, aqueous complexation, and equilibrium precipitation reactions). Starting with a low metal input, we gradually increase the total metal concentration and allow CCBATCH to compute the chemical equilibrium for each total-metal addition. To assess detoxification by the ligands, we assume that the toxic Zn species is free Zn, considered to have a toxicity-threshold value of 3.4 μM, based on a study with a *Desulfovibrio desulfuricans* culture (Sani et al. 2001).

We perform the three numerical metal-titration experiments listed in Table 8 to show the incremental effect on detoxification of: (1) only inorganic freshwater constituents; (2) adding 20 mg VSS/l of active cells or inert biomass (1.77×10^{-4} M), and 20 mg VSS/l of EPS (1.77×10^{-4} M); and (3) also adding 0.33 mg/l sulfide (10^{-5} M). The biomass concentrations are representative of sulfidic permeable reactive barriers when particulate organic matter hydrolysis limits biodegradation (Schwarz and Rittmann 2007).

Figures 3–5 show the evolution of Zn speciation during each metal titration. In Fig. 3, inorganic freshwater constituents barely affect Zn speciation, and free Zn is the dominant Zn species over almost all the tested concentration range, except at high added Zn concentrations, when $ZnCO_{3(s)}$ precipitates. Figure 4 shows that biomass complexes control Zn speciation in the Zn concentration range of 10^{-10}–10^{-4} M, inducing

Table 7 Reactive ligands generated from 1 mol of glucose

Ligand type	Yield coefficient	Biomass yield[a] mol/mol-glucose	Reactive-ligand density[b] mol/mol-biomass	Reactive-ligand yield mol/mol-glucose
Active cells	0.53	0.190	0.316	0.06
EPS	0.37	0.132	0.762	0.10
SMP	0.10	0.036	0.281	0.01
Sulfide	–	–	–	2.11
Total	1.00	0.358	–	2.28

[a] Using the stoichiometry of microbial product generation of Table 6

[b] Reactive sites include carboxyl and phosphoryl sites only. Site densities in mol/g (dry wt) were multiplied by [113 g (dry wt)/mol-biomass] to obtain site densities in mol/mol-biomass

Table 8 Windows of total-Zn concentration (μM), for the conditions of Figs. 1, 2 and 3, in which ligands present in the biogeochemical framework achieve Zn detoxification, or free-$Zn^{2+} \leq 3.4$ μM

Case number	Inorganic complexes[a]	Biomass-associated complexes[b]	Sulfide complexes[c]	Total-Zn window (μM)
1	Yes	No	No	3.4–4 (Fig. 1)
2	Yes	Yes	No	3.4–23 (Fig. 2)
3	Yes	Yes	Yes	3.4–36 (Fig. 3)

[a] Due to typical freshwater constituents

[b] Due to 20 mg VSS/l of active cells or inert biomass, and 20 mg VSS/l of EPS

[c] Due to 0.33 mg/l sulfide

a 100-fold decrease in free Zn concentration. Additionally, at 10^{-5} M added Zn, surface sites on biomass show signs of saturation, and the Zn^{2+} curve experiences a slope increase, reaching afterwards a plateau in the high-added Zn region, when $ZnCO_{3(s)}$ precipitates form. On the other hand, speciation results including all ligands (Fig. 5) show that Zn speciation is controlled by different ligands, depending on Zn concentration. With increasing added Zn concentration, Zn speciation is successively controlled by Zn-inorganic complexes, $ZnS_{(s)}$, Zn-cell complexes, free Zn, $ZnCO_{3(s)}$, and free Zn. Fig. 5 exemplifies how coordination by sulfide controls Zn speciation as long as total sulfide is greater than added Zn. Starting at a concentration of added Zn of

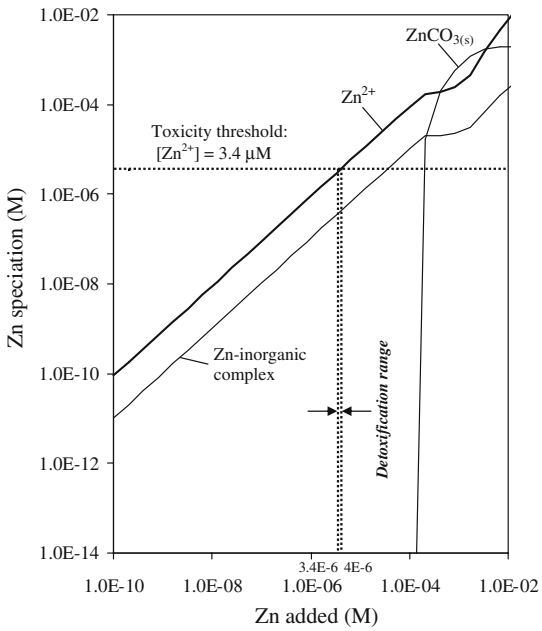

Fig. 3 Zn titration of freshwater. Freshwater conditions are pH = 7, $[Na^+] = 2.5 \times 10^{-4}$ M, $[Ca^{2+}] = 1 \times 10^{-3}$ M, $[Mg^{2+}] = 3 \times 10^{-4}$ M, $[SO_4^{2-}] = 3 \times 10^{-4}$ M, $[Cl^-] = 2.5 \times 10^{-4}$ M, and $[CO_3^{2-}] = 2 \times 10^{-3}$ M. Zn-inorganic complexes include Zn complexes with hydroxide, sulfate, carbonate, and chloride. We considered all possible equilibrium complexes and acid/base species and used critically reviewed values for equilibrium constants (NIST 1997)

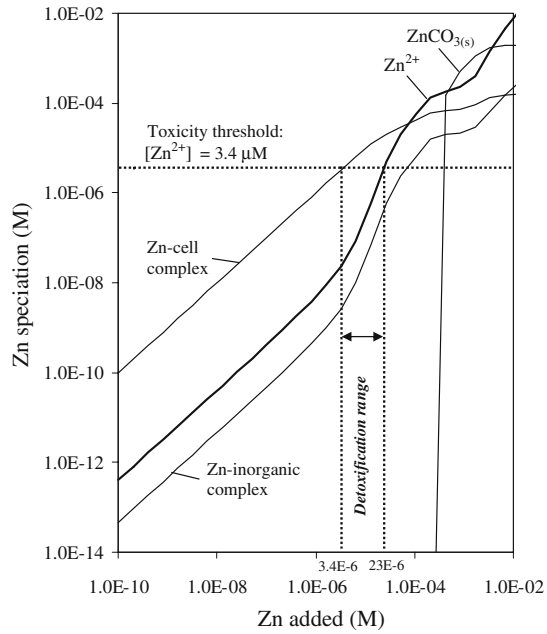

Fig. 4 Zn titration of freshwater in the presence of active cells or inerts 1.77×10^{-4} M and EPS 1.77×10^{-4} M only and not sulfide. Freshwater conditions are pH = 7, $[Na^+] = 2.5 \times 10^{-4}$ M, $[Ca^{2+}] = 1 \times 10^{-3}$ M, $Mg^{2+}] = 3 \times 10^{-4}$ M, $[SO_4^{2-}] = 3 \times 10^{-4}$ M, $[Cl^-] = 2.5 \times 10^{-4}$ M, and $[CO_3^{2-}] = 2 \times 10^{-3}$ M. Zn-inorganic complexes include Zn complexes with hydroxide, sulfate, carbonate, and chloride; Zn-cell complexes include Zn complexes with surface functional groups on active cells or inerts and EPS. We considered all possible equilibrium complexes and acid/base species and used critically reviewed values for equilibrium constants (NIST 1997)

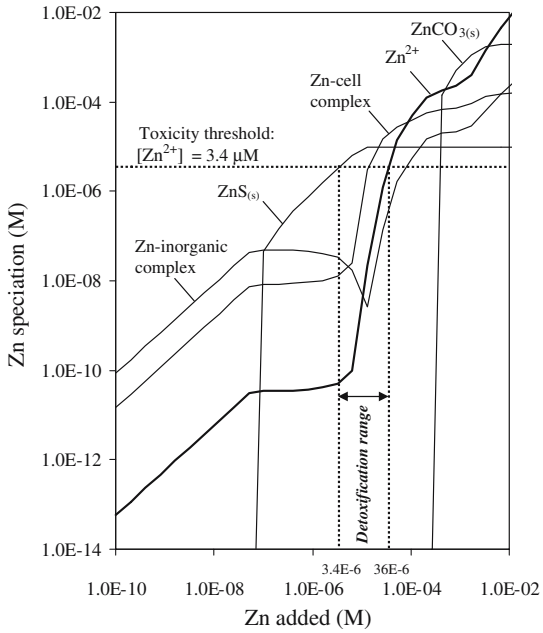

Fig. 5 Zn titration of freshwater in the presence of sulfide (10^{-5} M), active cells or inerts 1.77×10^{-4} M, and EPS 1.77×10^{-4} M. Freshwater conditions are pH = 7, $[Na^+] = 2.5 \times 10^{-4}$M, $[Ca^{2+}] = 1 \times 10^{-3}$ M, $[Mg^{2+}] = 3 \times 10^{-4}$ M, $[SO_4^{2-}] = 3 \times 10^{-4}$ M, $[Cl^-] = 2.5 \times 10^{-4}$ M, and $[CO_3^{2-}] = 2 \times 10^{-3}$ M. Zn-inorganic complexes include Zn complexes with hydroxide, sulfide, sulfate, carbonate, and chloride; Zn-cell complexes include Zn complexes with surface functional groups on active cells or inerts and EPS. We considered all possible equilibrium complexes and acid/base species and used critically reviewed values for equilibrium constants (NIST 1997)

10^{-5} mol/l, equal to the total H_2S concentration present, the free Zn concentration experiences a rapid increase spanning 7 orders of magnitude from 10^{-11} to 10^{-4} M. When Zn is primarily coordinated to sulfide, either as aqueous complex or forming a sulfide solid, it is effectively detoxified, or maintained below the toxicity threshold of 3.4 μM. Also, sulfide concentrations in natural or engineered systems can be much higher than the assumed 10^{-5} M. Increasing total sulfide would have the effect of extending the Zn^{2+} plateau to the right in Fig. 5.

To assess quantitatively how the incremental addition of ligands affects detoxification, we compute the detoxification range directly from the titration figures. The detoxification range is the window of total Zn that is detoxified by ligands present in the system. The lower bound of the detoxification range corresponds to the total added Zn concentration equal to the toxicity threshold of 3.4 μM, representing the imaginary case in the absence of ligands, even water, when all Zn is present as free Zn. Then, when ligands are present, the upper bound of the detoxification range corresponds to the total added Zn concentration that gives a free Zn concentration equal to the toxicity threshold of 3.4 μM. By reducing the free-Zn concentration, an increased presence of ligands and higher Zn affinities expand the Zn-detoxification range.

The detoxification range information is summarized in Table 8. Zn forms few hydrolysis products and complexes weakly with typical freshwater ligands (SO_4^{2-}, CO_3^{2-}, HCO_3^- and Cl^-). Accordingly, Case 1 shows a very small detoxification range of 3.4–4 μM. The carboxyl and phosphoryl functional groups on biomass have significantly higher affinities for Zn than typical freshwater ligands, and, hence, Case 2 has a much higher detoxification range of 3.4–23 μM. Finally, sulfide has the highest affinity for Zn among all ligands, extending the detoxification range considerably further in Case 3: 3.4–36 μM.

Thus, sulfide shows great detoxification potential, because detoxification is possible over a large metal concentration range as long as total sulfide is greater than total Zn. On the other hand, biomass also shows some detoxification potential in the absence of sulfide; however, detoxification is constrained to a rather narrow metal concentration range.

While important and generalizable conclusions can be drawn from the speciation analyses presented here, it is important to point out their limitations. Speciation analyses are only a snapshot in time of a system's condition. They do not consider the system's dynamics, and as such do not convey information on how a system is evolving. The more complete biogeochemical analyses, which consider the temporal and spatial effects of biological and physical processes, are presented in our companion paper (Schwarz and Rittmann 2007). Nevertheless, the results from the biogeochemical analysis are relevant to find good simplifying assumptions and to interpret numerical modeling results in more complex settings.

Discussion

Cells oxidize themselves to meet maintenance-energy needs, and the decrease in cell mass is often represented as endogenous decay (Rittmann and McCarty 2001). However, not all the decayed biomass is oxidized and a small portion accumulates as biomass debris or inert biomass. Although all biomass is ultimately biodegradable, the inert fraction can be considered refractory to further biological attack in most biochemical settings due to its low biodegradation rate (Grady et al. 1999). Only in situations with no alternative loss processes working might it be necessary to include the very slow biodegradation of inerts.

Bound EPS are dissolved or hydrolyzed slowly by enzymes released when bacteria lyse (Sutherland 1999; Davies 1999). The unified theory of bacterial products (Laspidou and Rittmann 2002a, b) proposes that this is the only significant source of BAP. Others call the EPS-cleavage products soluble EPS (Nielsen et al. 1997; Hsieh et al. 1994), and soluble EPS is effectively the same as BAP in the unified model. SMP are important because they form the majority of the dissolved organic matter in many cases and also can complex metals (Rittman and McCarty 2001). Laspidou and Rittmann (2002b) found that BAP was the dominant SMP component, because UAP is biodegraded considerably faster than BAP. However, despite its significance, BAP formation/EPS hydrolysis kinetics is poorly characterized and available parameters (Rittman and McCarty 2001; Laspidou and Rittmann 2002b) are system specific.

It is necessary to use empirical chemical formulas for cells in the balancing of biological reactions. We use the widely accepted empirical formula $C_5H_7O_2N$ (Rittmann and McCarty 2001), but the relative proportion of elements actually present in cells depends on the microorganisms involved and their growth conditions. For example, the nitrogen content of cells averages 12 percent as in $C_5H_7O_2N$, although it varies between 6% and 15% (Rittmann and McCarty 2001). Hence, one empirical formula will not be exactly applicable to all situations, but the theoretical concepts used to build the matrix of stoichiometry (Table 1) are still valid (Grady et al. 1999).

Surface complexation models accounting for three conceptual reactive sites can be used to fit the acid/base behavior of cell suspensions (Yee and Fein 2001; Songkasiri et al. 2002). On the basis of the fitted pK_a values, the dominant reactive sites are considered to be carboxyl, phosphoryl, and amino and/or hydroxyl groups. However, the direct analysis of the bacterial cell surface is required for confirming the existence of these surface functional groups (Guiné et al. 2006). Importantly, the generalized model of Yee and Fein (2001) stands out among surface-complexation models because it is applicable to complex bacterial mixtures. Surprisingly, despite their different envelope structure, the metal sorption capacity and reactivity of Gram-positive and Gram-negative bacteria mixtures are similar (Yee and Fein 2003). Despite its apparently wide applicability, the generalized sorption model in complex natural systems, such as sulfidic communities, must be tested and quantified further.

Stability-constant information for bacterial products is very limited. Because of the lack of this critical information, we assumed that zinc binding to EPS and BAP can be described using stability constants valid for cell-walls. Songkasiri et al. (2002) found that pK_a values for *S. alga* cell walls and EPS were similar, indicating that microbial products might have dominant functional groups with nearly identical reactivity. Yee and Fein (2003) also found that stability constants determined for bacterial mixtures and for *B. subtilis* are comparable.

EPS have been found to play a dominant role in metal sorption (Guiné et al. 2006); however, the processes that control EPS composition are not well understood (Wingender et al. 1999). Exopolysaccharides were initially identified as the most abundant constituents of EPS. However, proteins and nucleic acids can also appear in significant amounts or even predominate (Wingender et al. 1999). The reactivity of EPS is due to their polyanionic nature. Several amino acids are negatively charged in extracellular proteins (Wingender et al. 1999) and exopolysaccharides have uronic acids or ketal-linked pyruvate (Sutherland 2001). Not surprisingly then, the EPS reactive-site densities show the greatest variance among microbial products. Since EPS can consti-

tute as much as 50–90% of the total dry weight of cells (Christensen and Characklis 1990; Nielsen et al. 1997), an improved understanding of EPS is key to advance mechanistic models on the fate of metals in complex microbial systems.

It is often assumed that basic hydroxyl and amino sites do not complex with metals significantly, because protons out-compete metals on these acid–base sites at typical pH values. For example, Zn complexes with carboxyl and phosphoryl sites accounted for all metal adsorption onto *B. subtilis* over the pH range from 2 to 8 (Fein et al. 2001). However, at higher pH values, binding onto amino or hydroxyl sites will eventually become significant as these sites deprotonate (Songkasiri et al. 2002; Guiné et al. 2006).

In natural and engineered systems, the ligand concentrations can vary significantly, potentially influencing the detoxification ranges. For situations similar to Case 1, when detoxification is by inorganic constituents only, the detoxification range is not expected to vary significantly, because Zn speciation is barely affected by this type of ligands for typical freshwater conditions. For scenarios similar to Case 3, significantly higher detoxification ranges can be expected, because sulfide concentrations can vary over several orders of magnitude in natural and engineered systems. For example, Benner et al. (1999) measured within a sulfidic PRB a sulfide concentration of 30 mg/l, two orders of magnitude higher than the value assumed in our analysis.

Conclusions

We developed a biogeochemical framework for understanding and quantitatively evaluating metals bio-protection in sulfidic microbial systems. We implemented the biogeochemical framework by adding to the biogeochemical model CCBATCH expanded sub-models for surface complexation and the formation of soluble and solid products. We applied an expanded CCBATCH to understand the relative importance of the various key ligands of sulfidic systems in Zn detoxification. The key outcome of the biogeochemical analyses is that sulfide has the greatest detoxification potential among all reactive ligands of sulfidic systems and can be effective in detoxifying Zn under a wide range of geochemical conditions. This outcome is explained by the relative affinities of the various ligands toward Zn and by the estimates of their concentrations for sulfidic systems. Moreover, the relevance of sulfide as a detoxifying agent should become even higher if a dynamic setting is considered, because sulfide is continually generated at the highest rate among all reactive ligands and is also the most mobile ligand. Thus, the rate of production— as well as the affinity toward the metal—is key to bio-protection.

References

Allen HE, Hansen DJ (1996) The importance of trace metal speciation to water quality criteria. Water Environ Res 68(1):42–53

Banaszak JE, van Briesen JM, Rittmann BE, Reed DT (1998) Mathematical modeling of the effects of aerobic and anaerobic chelate biodegradation on actinide speciation. Radiochim Acta 82:445–451

Barnes LJ, Jansen FJ, Scheeren PJH, Versteegh JH, Koch RO (1991) Simultaneous microbial removal of sulfate and heavy metals from wastewater. Paper presented at the 1st European Metals Conference, Bruxelles, Belgium

Benner SG, Blowes DW, Gould WD, Herbert RB Jr, Ptacek CJ (1999) Geochemistry of a permeable reactive barrier for metals and acid mine drainage. Environ Sci Technol 33(16):2793–2799

Brown PL, Markich SJ (2000) Evaluation of the free ion activity model of metal-organism interaction: extension of the conceptual model. Aquatic Toxicol 51:177–194

Campbell PGC (1995) Interactions between trace metals and organisms: critique of the free-ion activity model. In: Tessier A, Turner D (eds) Metal speciation and bioavailability in aquatic systems. Wiley, Chichester, UK

Campbell PGC, Errecalde O, Fortin C, Hiriart-Baer VP, Vigneault B (2002) Metal bioavailability to phytoplankton—applicability of the biotic ligand model. Comp Biochem Physiol Part C 133:189–206

Christensen BE, Characklis WG (1990) Physical and chemical properties of biofilms. In: Characklis WG, Marshall KC (eds) Biofilms. Wiley, New York

Cox JS, Smith DS, Warren LA, Ferris FG (1999) Characterizing heterogeneous bacterial surface functional groups using discrete affinity spectra for proton binding. Environ Sci Technol 33(24):4514–4521

Daskalakis KD, Helz GR (1993) The solubility of sphalerite (ZnS) in sulfidic solutions at 25°C and 1 atm pressure. Geochim Cosmochim Acta 57:4923–4931

Davies DG (1999) Regulation of matrix polymer in biofilm formation and dispersion. In: Wingender J, Neu TR, Flemming HC (eds) Microbial extracellular polymeric substances: characterization, structure and function. Springer-Verlag Berlin Heidelberg

De Filippi LJ (2000) Sulfate-reducing bacteria and other biological agents for bioremediation of hexavalent chromium and other heavy metals. In: Wise LW (ed) Bioremediation of contaminated soils. Marcel Dekker, New York

Dzombak DA, Morel FMM (1990) Surface complexation modeling. John Wiley & Sons, New York

Fein JB, Martin AM, Wightman PG (2001) Metal adsorption onto bacterial surfaces: development of a predictive approach. Geochim Cosmochim Acta 65:4267–4273

Fenchel T, Finlay BJ (1995) Ecology and evolution in anoxic worlds. Oxford University Press, New York

Flemming HC, Wingender J (2001) Relevance of microbial extracellular polymeric substances (EPSs)-Part I: structural and ecological aspects. Water Sci Technol 43(6):1–8

Gambrell RP (1994) Trace and toxic metals in wetlands-a review. J Environ Qual 23:883–891

Grady CPL Jr, Daigger GT, Lim HC (1999) Biological wastewater treatment, 2nd edn. Marcel Dekker Inc, New York

Guiné V, Spadini L, Sarret G, Muris M, Delolme C, Gaudet JP, Martins JMF (2006) Zinc sorption to three Gram-negative bacteria: combined titration, modeling, and EXAFS study. Environ Sci Technol 40:1806–1813

Hsieh KM, Murgel GA, Lion LW, Shuler ML (1994) Interactions of microbial biofilms with toxic trace metals 1. Observation and modeling of cell growth, attachment, and production of extracellular polymer. Biotechnol Bioeng 44:219–231

Kim CS, Zhou QH, Deng BL, Thornton EC, Xu HF (2001) Chromium(VI) reduction by hydrogen sulfide in aqueous media: stoichiometry and kinetics. Environ Sci Technol 35:2219–2225

Kuo WC, Parkin GF (1996) Characterization of soluble microbial products from anaerobic treatment by molecular weight distribution and nickel-chelating properties. Water Res 30(4):915–922

Laspidou CS, Rittmann BE (2002a) A unified theory for extracellular polymeric substances, soluble microbial products, and active and inert biomass. Water Res 36:2711–2720

Laspidou CS, Rittmann BE (2002b) Non-steady state modeling of extracellular polymeric substances, soluble microbial products, and active and inert biomass. Water Res 36:1983–1992

Liu H, Fang HHP (2002) Characterization of electrostatic binding sites of extracellular polymers by linear programming analysis of titration data. Biotechnol Bioeng 80(7):806–911

Lloyd JR, Mabbett AN, Williams DR, Macaskie LE (2001) Metal reduction by sulfate-reducing bacteria: physiological diversity and metal specificity. Hydrometal 59:327–337

Madigan MT, Martinko JM, Parker J (2000) Brock biology of microorganisms, 9th edn. Prentice-Hall, New Jersey

Morel FFM, Hering JG (1993) Principles and applications of aquatic chemistry. John Wiley & Sons, New York

Nielsen PH, Jahn A, Palmgren R (1997) Conceptual model for production and composition of exopolymers in biofilms. Water Sci Technol 36:11–19

NIST (1998) Critically selected stability constants of metal complexes database, Version 5.0

Noguera DR, Araki N, Rittmann B (1994) Soluble microbial products (SMP) in anaerobic chemostats. Biotechnol Bioeng 44:1040–1047

Paquin PR, Gorsuch JW, Apte S et al (2002) The biotic ligand model: a historical overview. Comp Biochem Physiol Part C 133:3–35

Rittmann BE, van Briesen JM (1996) Microbiological processes in reactive transport modeling. Rev Mineral 34:311–334

Rittmann BE, McCarty PL (2001) Environmental biotechnology: principles and applications. McGraw-Hill, New York

Rittmann BE, Banaszak JE, Reed DT (2002a) Reduction of Np(V) and precipitation of Np(IV) by an anaerobic microbial consortium. Biodegrad 13:329–342

Rittmann BE, Banaszak JE, Van Briesen JM, Reed DT (2002b) Mathematical modeling of precipitation and dissolution reactions in microbiological systems. Biodegrad 13:239–250

Rickard D (1995) Kinetics of FeS precipitation: Part 1. Competing reaction mechanisms. Geochim Cosmochim Acta 59(21):4367–4379

Sani RK, Peyton BM, Brown LT (2001) Copper-induced inhibition of growth of *Desulfovibrio desulfuricans G20*: assessment of its toxicity and correlation with those of zinc and lead. Appl Environ Microbiol 67(10):4765–4772

Schwarz AO, Rittmann BE (2006) Analytical-modeling analysis of how pore-water gradients of toxic metals confer community resistance. Adv Water Res (in press)

Schwarz AO, Rittmann BE (2007) Modeling bio-protection and the gradient resistance mechanism using CCBATCH. Biodegrad (in press). DOI 10.1007/s10532-007-9106-x

Songkasiri W, Reed DT, Rittmann BE (2002) Biosorption of neptunium(V) by *Pseudomonas fluorescens*. Radiochim Acta 90:785–789

Songkasiri W (2003) Biological processes in nuclear waste treatment: bio-sorption and bio-reduction of actinides. Dissertation, Northwestern University

Songkasiri W, Willett A, Reed DT, Rittmann BE, Koenigsberg S (2004) Bioremediation of neptunium(V) using lactate, hydrogen (H2), or hydrogen release compound (HRC). In: Proceedings of the 2003 Battelle symposium on in situ and on site bioremediation, Orlando, FL, June 2003

Stone AT (1997) Reactions of extracellular organic ligands with dissolved metal ions and mineral surfaces. Rev Mineral 35:309–344

Stumm W, Morgan JJ (1996) Aquatic Chemistry. John Wiley & Sons, New York

Sutherland IW (1999) Biofilm polysaccharides. In: Wingender J, Neu TR, Flemming HC (eds) Microbial extracellular polymeric substances: characterization, structure and function. Springer-Verlag Berlin Heidelberg

Sutherland IW (2001) Biofilm exopolysaccharides: a strong and sticky framework. Microbiol 147:3–9

Tebo BM, Obraztsova AY (1998) Sulfate-reducing bacterium grows with Cr(VI), U(VI), Mn(IV), and Fe(III) as electron acceptors. FEMS Microbiol Lett 162:193–198

Van Briesen JM, Rittmann BE (1999) Modeling speciation effects on biodegradation in mixed metal/chelate systems. Biodegradation 10(5):315–330

Van Briesen JM, Rittmann BE (2000) Mathematical description of microbiological reactions involving intermediates. Biotechnol Bioeng 67(1):35–52

Van Briesen JM, Rittmann BE, Xun L, Girvin DC, Bolton H Jr (2000) The rate-controlling substrate of nitrilotriacetate for biodegradation by Chelatobacter heintzii. Environ Sci Technol 34:3346–3353

White C, Gadd GM (1998) Reduction of metal cations and oxyanions by anaerobic and metal-resistant microorganisms: chemistry, physiology, and potential for the control and bioremediation of toxic metal pollution. In: Horikoshi K, Grant WD (eds) Extremophiles: microbial life in extreme environments. Wiley & Sons, New York

Webb JS, McGinness S, Lappin-Scott HM (1998) Metal removal by sulfate-reducing bacteria from natural and constructed wetlands. J Appl Microbiol 84:240–248

White C, Sharman AK, Gadd GM (1998) An integrated microbial process for the bioremediation of soil contaminated with toxic metals. Nat Biotechnol 16:572–575

Widdel F (1988) Microbiology and ecology of sulfate- and sulfur-reducing bacteria. In: Zehnder AJB (ed) Biology of anaerobic microorganisms. John Wiley & Sons, New York, pp 1–2

Willett AI, Rittmann BE (2003) Slow complexation kinetics for ferric iron and EDTA complexes make EDTA non-biodegradable. Biodegradation 4(2):105–121

Wingender J, Neu TR, Flemming HC (1999) What are bacterial extracellular polymeric substances. In: Wingender J, Neu TR, Flemming HC (eds) Microbial extracellular polymeric substances: characterization, structure and function, Springer-Verlag Berlin Heidelberg

Yee N, Fein JB (2001) Cd adsorption onto bacterial surfaces: a universal adsorption edge? Geochim Cosmochim Acta 65(13):2037–2042

Yee N, Fein JB (2003) Quantifying metal adsorption onto bacterial mixtures: a test and application of the surface complexation model. Gemicrobiol J 20:43–60